


Use of information-fusion deep-learning techniques to detect possible electricity theft: A proposed method


Maria Gabriel Chuwa

PhD candidate, College of Informatics and Virtual Education, University of Dodoma, Tanzania

 <https://orcid.org/0000-0002-7192-9584>


Daniel Ngondya

Lecturer, College of Informatics and Virtual Education, University of Dodoma, Tanzania

 <https://orcid.org/0000-0003-4267-6351>

Rukia Mwifunyi

Lecturer, College of Informatics and Virtual Education, University of Dodoma, Tanzania

 <https://orcid.org/0000-0001-7465-3926>

Abstract

The performance of electricity utilities in many African countries is undermined by electricity theft. Such non-technical losses (NTLs) pose significant economic challenges to electricity grids, leading to the need for improved detection methods. This study tested an NTL detection method that transformed electricity consumption (EC) profiles into two-dimensional (2D) and one-dimensional (1D) representations, and utilised deep-learning techniques, specifically convolutional neural networks (CNN) and multi-layer perceptron (MLP), to extract features indicating NTLs. This NTL detection method involved three parallel branches: analysing temporal information from application of a Markov transition field (MTF) to EC patterns; analysing spectral information from application of the continuous wavelet transform (CWT) tool; and extracting frequent co-occurrence features from 1D consumption patterns. CNN and MLP were employed within the three branches to capture information from the 2D and 1D inputs, respectively. The features extracted from the three branches were then aggregated through information fusion and applied to EC datasets produced by the State Grid Corporation of China (SGCC) and the Irish Commission for Energy Regulation (CER). This multi-branch approach was found to offer strong NTL detection accuracy. With the SGCC dataset, the method achieved an AUC (area under the curve) of 96.7%, a mAP@100 (mean average precision at 100) of 95.7%, and an FPR (false positive rate) of 8.1%. With the CER dataset, the method achieved an AUC of 96.7%, a mAP@100 of 97.3%, and an FPR of 5.2%.

Keywords

electricity consumption (EC), electricity theft, non-technical losses (NTLs), information fusion, deep-learning, convolutional neural networks (CNN), multi-layer perceptron (MLP), Markov transition field (MTF), continuous wavelet transform (CWT)

DOI: <https://doi.org/10.23962/ajic.i35.20652>

Recommended citation

Chuwa, M.G., Ngondya, D., & Mwifunyi, R, (2025). Use of information-fusion deep-learning techniques to detect possible electricity theft: A proposed method. *The African Journal of Information and Communication (AJIC)*, 35, 1-16. <https://doi.org/10.23962/ajic.i35.20652>



This article is licensed under a Creative Commons Attribution 4.0 International (CC BY 4.0) licence:
<https://creativecommons.org/licenses/by/4.0>

1. Introduction

In many African countries, the performance and financing of the electricity grid are undermined by high rates of theft. In South Africa, it is estimated that 32% of transmitted electricity is stolen, while in Nigeria, electricity theft is thought to range between 32% to 34% of national transmissions annually (Adongo et al., 2021). Other parts of the world also suffer from high levels of electricity theft. For example, in China, an estimated 16% of generated electricity is stolen, while India and Brazil lose around 25% and 15% of their annual production, respectively (J. Chen et al., 2023). Yan and Wen (2022) point out that electricity theft is one of the main causes of financial difficulties faced by electricity utilities in both the developing and developed world. In addition to the financial impact, electricity theft also leads to risks to public safety, power surges, network damage, and degraded reliability. It is, thus, critical that electricity utilities detect non-technical losses (NTLs) as accurately as possible, so as to be alerted to possible electricity theft (Y. Chen et al., 2023).

In recent years, detection and prevention of electricity theft have received growing attention from researchers and industry practitioners. Conventional machine-learning methods, which rely on feature engineering, have been widely explored and reported to achieve acceptable results in identifying instances of electricity theft (Guarda et al., 2023). These machine-learning-based approaches typically involve extracting a variety of features, such as statistical metrics (e.g., maximum, minimum, mean, and standard deviation), frequency domain characteristics, electricity measurement data (e.g., phase imbalance, power factor), and static information related to geographic location, economic activity, and weather conditions (Chuwa & Wang, 2021). These features are classified using conventional machine-learning algorithms, including support vector machines (SVMs), k-nearest neighbours (KNNs), decision trees, and gradient-boosting methods. For example, Fang et al. (2023) proposed a light gradient-boosting method with 56 statistical features for detection of electricity theft. Zidi et al. (2023) incorporated 10 different electricity features and categorical features to detect theft using five machine-learning techniques: SVMs, KNNs, decision trees, random forest, bagging ensemble, and artificial neural networks (ANNs).

While conventional machine-learning-based methods have demonstrated promising performance in electricity theft detection, they have certain limitations. They primarily depend on human expertise and intervention for crucial feature-extraction and feature-engineering tasks. Handcrafted feature-engineering can lead to important information being missed, thus potentially reducing the effectiveness of conventional machine-learning techniques in accurately detecting electricity theft.

Deep-learning approaches to detecting electrical NTLs

Recently, to address the limitations of conventional machine-learning approaches, researchers have turned to deep-learning methods, which have the ability to extract relevant features automatically. Shi et al. (2023) proposed an approach that uses a transformer neural network (TNN) with a conv-attentional module to extract global and local features. Bai et al. (2023) proposed a hybrid convolutional neural network (CNN)-transformer model to detect electrical NTLs. Their work used a CNN with dual scale and dual branch architecture to extract multi-scale features in a local-to-global fashion. In addition, a transformer model with Gaussian weighting was used to capture the temporal dependence of electricity consumption (EC). In a study by Javaid et al. (2021), CNN, long short-term memory (LSTM), and a deep Siamese network were used to detect electricity theft in smart grids. The study used a CNN model and LSTM to extract features from weekly data and learning sequences from daily data, respectively. At the same time, a deep Siamese network was used to identify similarities between inputs by comparing feature vectors.

All of the aforementioned deep-learning studies extracted features from a 1D representation of the EC patterns. However, it has been found that feature extraction using CNN has a better outcome for 2D data than for 1D data (Nawaz et al., 2023). Extracting patterns directly from 1D time-series data can be difficult due to high variability and the lack of spatial structure (Haq et al., 2023). Encoding energy consumption data into 2D image-like formats enables CNN to capture local and temporal patterns more efficiently through shared convolutional kernels (Massaferro et al., 2022). To enhance the ability of CNN models to capture complex patterns in power consumption data, researchers have explored transforming 1D time-series signals into 2D representations.

For example, Nawaz et al. (2023) proposed a hybrid approach combining CNN with extreme gradient boosting (XGBoost) for electricity theft detection. Their method involved extracting features from energy consumption data in 1D and 2D formats, with weekly consumption data arranged into a matrix for 2D representation. Integrating XGBoost with a wide-and-deep CNN architecture significantly improved detection accuracy for electricity theft. Similarly, studies by Liao et al. (2023) and Xia et al. (2023) have demonstrated strong performance in feature extraction and NTL detection using CNN-based approaches on 2D representations of energy consumption data. Pan et al. (2023) also transformed consumption patterns into 2D image data—using Gramian angular field (GAF), Markov transition field (MTF), and recurrence plot techniques—and combined them into a three-channel image for input into a parallel convolutional neural network (PCNN) model. This architecture enhanced the CNN's capacity to extract robust features from high-dimensional data.

Information fusion

The above studies have demonstrated that representing the EC patterns in 2D formats has significantly enhanced NTL detection accuracy. However, not all characteristics can be adequately captured using one 2D representation alone. Accurately measuring factors such as periodic and recurrent patterns, and transient events, is critical to optimising CNN performance for NTL detection. According to our analysis of data-transformation methods in the existing literature, measuring such factors is most effective through information fusion, specifically by combining MTF and continuous wavelet transform (CWT) with CNN. In addition, our literature analysis found that raw 1D data representations yielded favourable results when processed using a multi-layer perceptron (MLP) model.

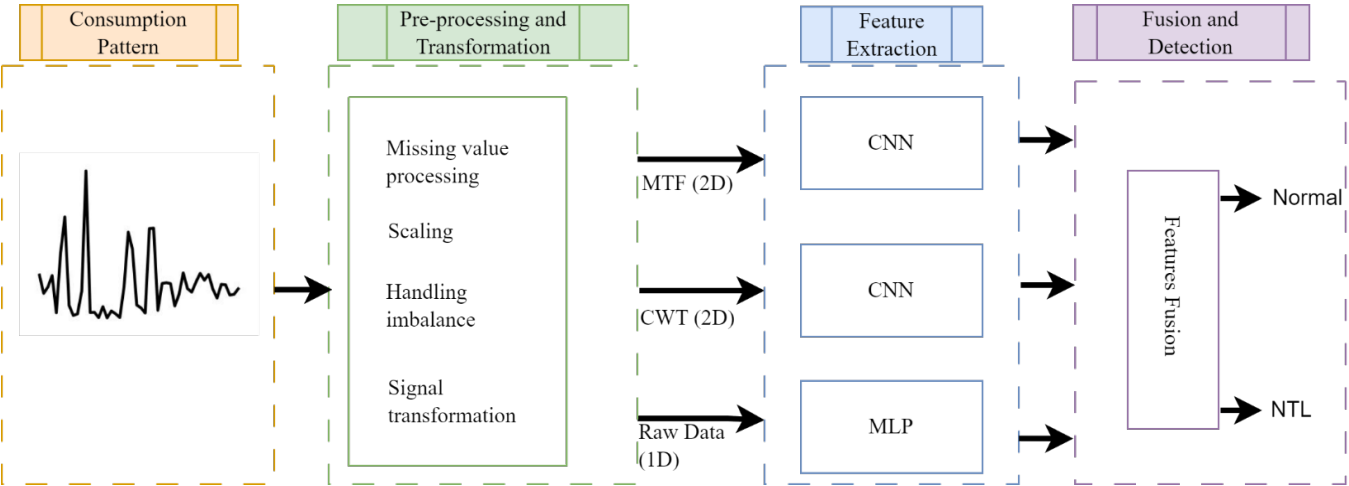
Accordingly, this study tested an information-fusion deep-learning method that extracted features from diverse EC pattern representations (CWT, MTF, and raw data) and fused the obtained features within a classifier for better detection performance. This proposed method was then evaluated using datasets produced by the State Grid Corporation of China (SGCC) and the Irish Commission for Energy Regulation (CER). We found that compared to other existing models, our method achieved superior performance. The main innovations in our proposed method are as follows:

- The method has three input branches: 2D inputs corresponding to CWT and MTF, and a 1D input for the raw EC series. This multi-modal representation captures the temporal, spectral, and periodic information of the adjacent EC pattern segments.
- Not relying on handcrafted features, the method utilises a combination of CNN and MLP deep-learning models to extract information from three input representations of EC. All the features from these three branches were then collated via information fusion using a simple feature concatenation scheme to support final NTL detection.

Framework for the proposed method

The framework for the proposed method consists of the following steps: (1) data pre-processing and transformation; (2) feature extraction and representation from the transformed data samples; (3) feature extraction from different input representations; and (4) fusion of features, by concatenation of features from different modalities, into a single vector for NTL detection. The framework is shown in Figure 1.

Figure 1: Framework



The remainder of this article is organised as follows: Section 2 describes the study’s data pre-processing and transformation activities; section 3 sets out the processes for feature extraction and fusion; section 4 presents the findings from evaluation of our proposed method; and section 5 provides conclusions.

2. Data pre-processing and transformation

Data pre-processing and transformation were fundamental to creating a usable data structure—a structure that enabled the proposed model to be trained and to generate reliable predictions.

CER dataset

The CER dataset (CER, 2012) provided by the Irish Social Science Data Archive (ISSDA) comprises EC data from over 5,000 residential and commercial electricity users. The data was recorded at half-hour intervals between July 2009 and December 2010. All customers for this dataset were considered legitimate, with no illegal electricity users. From the CER data samples, we generated attack samples. The six attack scenarios indicated in Table 1, defined by Jokar et al. (2016), were used to create attacks. The attack samples were generated from only 10% of the available load profiles by randomly selecting a subset of users and their load profiles. Each of the six attack-generation methods was applied to the selected users’ load profiles.

Table 1: Attacks and their definitions (from Jokar et al., 2016)

	Attack	Definition
1	$m_1(t) = \alpha e_t$ $0 < \alpha < 1$	Report a constant fraction of the energy consumed.
2	$m_2(t) = \beta_t e_t$ $\beta_t = \begin{cases} 0, & t_s < t < t_e \\ 1, & \text{else} \end{cases}$ <p>where, t_s is the time when the attack starts t_e is the time when the attack ends $t_e - t_s$ is randomly defined each day</p>	Report zero consumption at randomly defined times of the day.
3	$m_3(t) = \gamma_t e_t$ $0 < \gamma_t < 1$	Reduce consumption patterns by reporting less from time to time.
4	$m_4(t) = \gamma_t \cdot \text{mean}(e_t)$ $0 < \gamma_t < 1$	Report the consumption with reduced expected mean from time to time.
5	$m_5(t) = \text{mean}(e_t)$	Report constant consumption, which is the mean of day consumption.
6	$m_6(t) = e_{p-t}$ <p>p, is the total number of samples in a period to be reversed</p>	Reverse the order of measured values.

SGCC dataset

The SGCC dataset from China contains the daily recorded EC data of 42,372 electricity customers from January 2014 to October 2016 (SGCC, n.d.). The dataset is labelled and includes 3,615 real-world NTL scenarios.

Handling missing values

The pre-processing of real-world datasets often requires addressing missing or erroneous data. This study used the linear interpolation method described by Zheng et al. (2018) to estimate missing EC samples. This method is useful for time-series data as it captures the relationship between adjacent variables. Equation 1 below presents the mathematical formula of this method, where NaN represents a missing value, and x_i is consumption at time i .

$$x_i = \begin{cases} \frac{x_{i-1} + x_{i+1}}{2} & \text{if } x_i = \text{NaN}, x_{i-1}, x_{i+1} \neq \text{NaN} \\ 0 & \text{if } x_i = \text{NaN}, x_{i-1} \text{ or } x_{i+1} = \text{NaN} \\ x_i & \text{if } x_i \neq \text{NaN} \end{cases} \quad (1)$$

This study employed the three-sigma rule to systematically identify and rectify erroneous data samples. Observations were deemed to be outliers if they deviated beyond two standard deviations ($\pm 2\sigma$) from the mean of the data vector. Equation 2 presents the mathematical expression for correcting the erroneous data samples (Khan et al., 2020). In this Equation \bar{x} and σ_x represent the mean and standard deviation, respectively, of the consumption vector.

$$g(x_i) = \begin{cases} \bar{x} + 2\sigma_x, & \text{if } x_i > \bar{x} + 2\sigma_x \\ x_i, & \text{otherwise} \end{cases} \quad (2)$$

Data scaling

Since EC differs among customers, a min-max scaler was used to normalise the data, ensuring the data were on the same scale. The scaling process improves model performance and convergence while preventing bias from features with larger values. The min-max scaling is mathematically represented using Equation 3, where x_{min} and x_{max} represent the lowest and highest values in the data, respectively.

$$x' = \frac{x - x_{min}}{x_{max} - x_{min}} \quad (3)$$

Handling imbalance

One of the significant challenges in machine-learning models is the imbalance of data collected from smart meters. Typically, there are few records for classes with NTL, which leads to difficulties in training robust models. For example, in the SGCC dataset, $\approx 9\%$ of the data is labelled as theft scenarios. The class imbalance can reduce classification accuracy and create a bias towards the majority class. It is essential to balance the class distributions within the dataset to address the issues associated with class imbalance before training an NTL-detection model. In this study, we employed the synthetic minority over-sampling technique (SMOTE) proposed by Chawla et al. (2002). SMOTE addresses class imbalance by generating new samples and effectively handling imbalance for electricity theft detection (Pereira & Saraiva, 2021). It selects a minority sample and identifies neighbouring samples, and then creates synthetic instances through interpolation between these chosen samples.

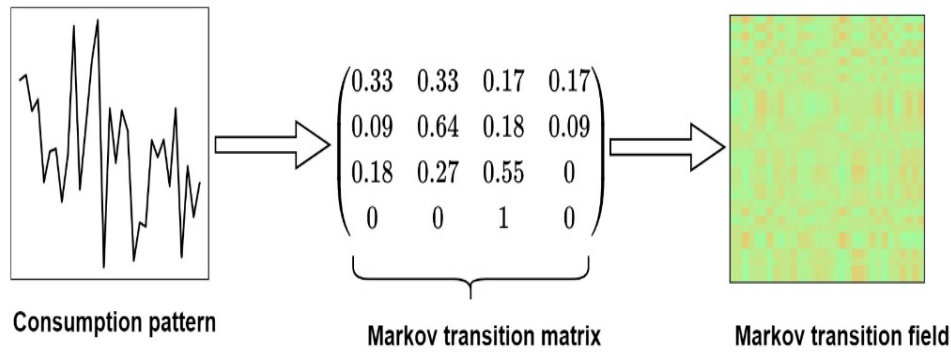
Data transformation

Our model processed EC data in multiple representations in order to capture diverse patterns within the data. A 2D structural representation was chosen to expose hidden temporal and spectral features suitable for CNN analysis. The preliminary experiments indicated that MTF (temporal representation) and CWT (time-frequency representation) yielded superior performance in detecting NTL compared to alternative 2D representations. Simultaneously, a raw 1D representation, which exposed frequent co-occurrence features of the EC data, demonstrated enhanced performance in NTL detection when analysed using MLP. Therefore, this study represented EC patterns using MTF, CWT and 1D raw representations in order to comprehensively capture the diverse characteristics of the EC data.

MTF

The Markov transition field visualisation technique transforms 1D time series data into a 2D image representation while preserving the information in the time domain. This transformation captures the first-order Markov transition probabilities among defined states, enhancing the ability to detect anomalies. For a consumption pattern denoted as $c_t = \{c_1, c_2, c_3, \dots, c_n\}$, state is identified, and each value c_t is allocated to a corresponding state s_j ($j \in [1, S]$). The Markov transition matrix M is constructed by calculating the frequency of transitions between these states, where p_{ij} of transitioning from state s_i to state s_j . This transition matrix, shown in Equation 4, highlights the relationships between data points in c_t and serves as a foundation for detecting anomalies that indicate electricity theft (Wang & Oates, 2015). The 2D representation facilitates the identification of unusual patterns and fluctuations that may signal fraudulent activity. Figure 2 illustrates the process of transforming the time series into an MTF.

$$M = \begin{vmatrix} p_{ij}|c_1 \in s_i, c_1 \in s_j & p_{ij}|c_1 \in s_i, c_2 \in s_j & \cdots & p_{ij}|c_1 \in s_i, c_n \in s_j \\ p_{ij}|c_2 \in s_i, c_1 \in s_j & p_{ij}|c_2 \in s_i, c_2 \in s_j & \cdots & p_{ij}|c_2 \in s_i, c_n \in s_j \\ \vdots & \vdots & \ddots & \vdots \\ p_{ij}|c_n \in s_i, c_1 \in s_j & p_{ij}|c_n \in s_i, c_2 \in s_j & \cdots & p_{ij}|c_n \in s_i, c_n \in s_j \end{vmatrix} \quad (4)$$

Figure 2: Process of transforming electricity consumption series to MTF

CWT

The continuous wavelet transform tool is a powerful approach to analysing time signals that provides a time–frequency representation. The ability of CWT to analyse signals with time-varying characteristics makes it ideal for detecting inconsistencies in EC patterns that might indicate theft. Electricity theft often manifests as unusual periodicities that are not reflected in the normal usage profile, and traditional time-domain or frequency-domain analyses struggle to capture this variation effectively. However, the CWT is highly effective at pinpointing these variations in time and frequency, enabling accurate identification. Consider a consumption pattern represented by the discrete sequence, $c_t = \{c_1, c_2, c_3, \dots, c_n\}$ and a wavelet function $\Psi(t)$. Then, the CWT is defined as a convolution between and wavelet , as expressed by Equation 5 (from Boashash, 2009).

$$CW(\tau, a) = \frac{1}{\sqrt{a}} \int_{-\infty}^{\infty} c_t \Psi^* \left(t - \frac{\tau}{a} \right) dt \quad (5)$$

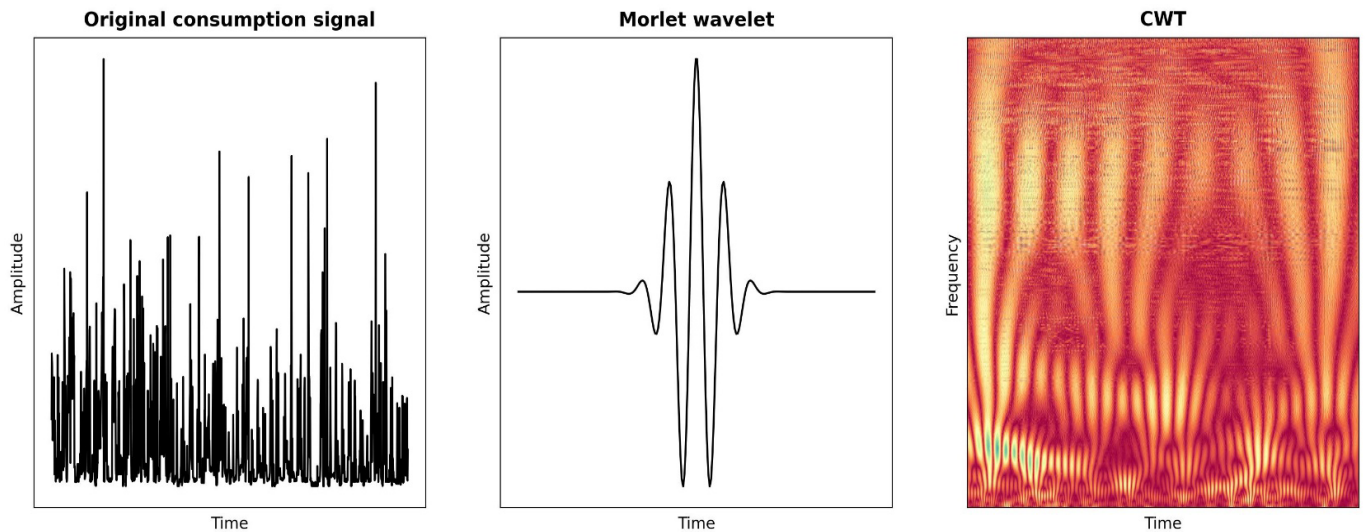
where $*$ denotes the complex conjugate of Ψ , τ represents the translation parameter controlling the wavelet's position in time, and $a = \omega_0/\omega$ is the scale parameter that controls the stretching of wavelets in time, narrowing it for large frequencies and widening it for small frequencies.

For a wavelet to be valid, it must have zero mean and be concentrated in both the time and frequency domains. A commonly used wavelet for spectral analysis is the Morlet wavelet, which we used in this study. It is defined in Equation 6 (V. C. Chen & Ling, 2002).

$$\Psi(t) = \pi^{-\frac{1}{4}} e^{-\frac{t^2}{2}} e^{-i\omega_0 t} \quad (6)$$

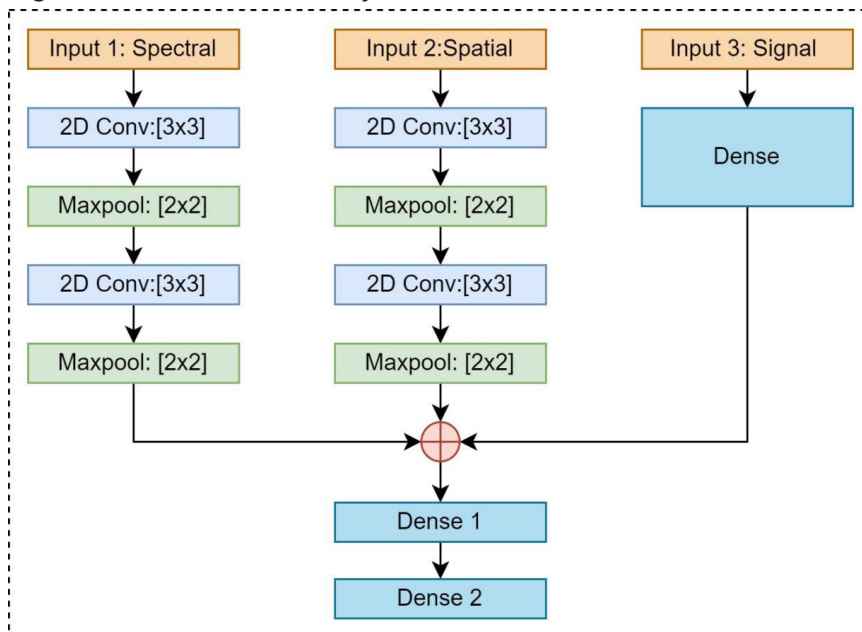
where ω_0 is central frequency.

The choice of ω_0 influences the time-frequency resolution of the analysis. A higher ω_0 provides better frequency resolution at the expense of time resolution. Figure 3 shows analysis of EC patterns using CWT with the Morlet wavelet.

Figure 3: Analysis of EC using CWT with the Morlet wavelet

3. Feature extraction and fusion

We used a deep neural network architecture (CNN and MLP) that allowed the model to learn from different types of data representations of the EC data: temporal (2D), spectral (2D), and raw data (1D), as presented in Figure 4.

Figure 4: Architecture of the joint feature extraction and classification model

The deep CNN feature-extraction component was constructed by two blocks of convolutional layers and two max-pooling layers. The convolutional layers learned to detect patterns and extract meaningful features from the 2D inputs. The convolution layer extracted features from the input by sliding multiple kernels (filters) over the input, generating feature maps that captured important spatial information.

The output of the convolutional operation can be expressed mathematically, as shown in Equation 7, where f_{ReLU} is the rectified linear unit (ReLU) activation function presented by Equation 8.

$$y_{(a,b)}^c = f_{\text{ReLU}} \left(b + \sum_i \sum_j X_{(i,j)} w_{(a-i,b-j)} \right) \quad (7)$$

$$f_{\text{ReLU}}(s_i) = \max(0, s_i) \quad (8)$$

After applying convolution and activation functions, the pooling process was applied to the feature maps. The pooling layers helped to reduce the dimensionality of the feature maps. We used the max-pooling operation, which takes the maximum value within a window in a feature map and is expressed by Equation 9.

Where y_i^p is the maximum value of in a window of size (m,n) ,

$$y_i^p = \max \left(y_{(m,n)}^c \right) \quad (9)$$

In the CNN feature-extraction component, convolutional and pooling operations worked alternately to capture the features from the two 2D representations of the EC patterns. Equations 10 and 11 express the overall process of feature extraction using convolution and pooling operations.

$$Y_{MTF} = y^p (y^c (y^p (y^c (X_{MTF})))) \quad (10)$$

$$Y_{CWT} = y^p (y^c (y^p (y^c (X_{CWT})))) \quad (11)$$

Further, the raw 1D input representation was passed through a dense network, as expressed in Equation 12. The dense network identified other information within the raw input that complemented the features extracted from the CWT and MTF inputs.

$$Y_{Raw} = f_{\text{ReLU}} \left(b + \sum_i X_{Raw,i} w_i \right) \quad (12)$$

After the feature extraction stage, the feature maps from the CNN of CWT and MTF inputs, and the dense representation for the raw input, were concatenated into a single feature vector, as expressed in Equation 13.

$$Y^t = Y_{MTF}^l \oplus Y_{CWT}^m \oplus Y_{Raw}^n \quad (13)$$

This feature-fusion step integrated the information from the different input representations, enabling the model to take advantage of various aspects of the data. The fused-feature vector was then passed through additional dense layers to further capture and learn the interactions between the combined feature representations.

4. Findings from evaluation of the proposed method

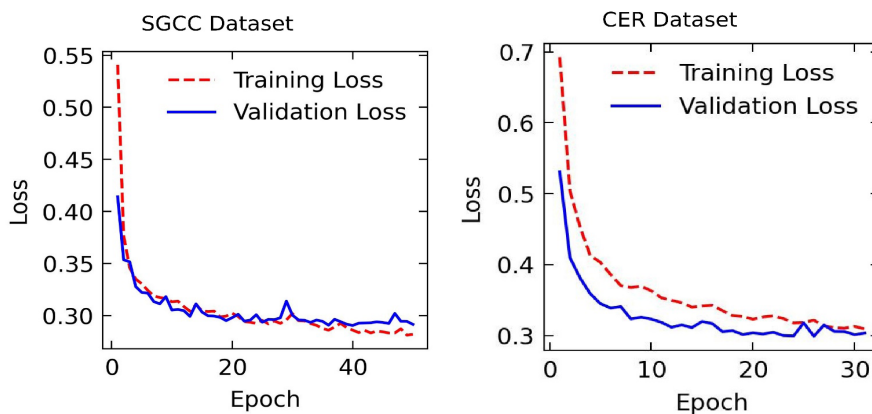
Training and validation

The multi-modal deep-learning architecture took three different types of inputs: a raw signal input, a 32x32 single-channel image input, and another 32x32 single-channel image input. The signal input was passed through a dense layer with 64 ReLUs (rectified linear units), while each image input went through a series of 2D convolutional and max-pooling layers to extract spatial features. The convolutional layers had 32 and 64 filters with 3x3 and 5x5 kernel sizes and ReLU activations. The max-pooling layers reduced the spatial dimensions of the feature maps.

Following the feature extraction for each modality, the outputs were concatenated into a single-feature vector. A dropout layer with a rate of 0.2 was then applied to the combined features to improve generalisation. The fused features vector was then passed through a dense layer of 128 units with ReLU activations. The final output layer utilised a softmax activation function to generate probability estimates for the two classes. The model parameters of all layers were then initialised randomly and trained by a back-propagation algorithm with ADAM (adaptive moment estimation). The ADAM minimises the loss function and updates the parameters during training to achieve effective model convergence.

Figure 5 provides the training loss and validation loss curves for the two datasets: SGCC and CER. Both datasets showed a general downward trend in training loss, indicating successful learning. However, the validation loss curves differed. The SGCC dataset exhibited less overfitting with a smaller gap between training and validation loss, suggesting better generalisation. Meanwhile, the CER dataset showed a more erratic validation loss curve, indicating potential difficulties in generalisation.

Figure 5: Training and validation loss curves for SGCC and CER datasets



Evaluation metrics

To enable a comprehensive performance evaluation, the study deployed widely used performance evaluation metrics, specifically area under the curve (AUC), mean average precision at M (MAP@M), and false positive rate (FPR). AUC measured the effectiveness of the method in distinguishing positive and negative instances. A high AUC would indicate the method's ability to effectively differentiate between classes and correctly identify the NTL cases. The MAP@M was used to assess the quality of the proposed method by evaluating its ability to identify NTLs among the top M electricity consumers. The formula for calculating MAP@M is illustrated in Equation 14, where P_i represents the precision of correctly identified NTL at a position i , and m denotes the total number of NTL samples among M labels.

$$MAP@M = \frac{1}{m} \sum_{i=1}^m P_i \quad (14)$$

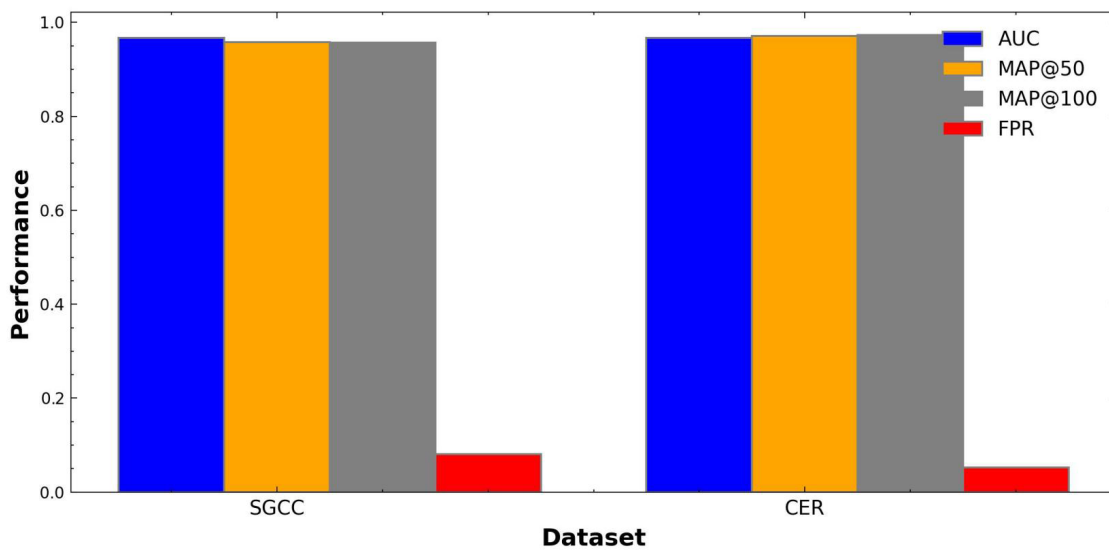
FPR represents the proportion of normal customers that the method incorrectly classified as abnormal, as defined in Equation 15, where FP and TN are the number of false positives and true negatives, respectively. A low FPR indicates good detection performance.

$$FPR = \frac{FP}{FP + TN} \quad (15)$$

Evaluation results

Figure 6 provides the results from the experimental evaluation of the proposed method on the SGCC and CER datasets. Four metrics, AUC, MAP@50, MAP@100, and FPR were used to assess the proposed model. As seen in the Figure 6, the method achieved impressive results for the CER dataset, with a MAP@50 of 97.1%, a MAP@100 of 97.3%, an AUC of 96.7%, and an FPR of 5.2%. These values indicate a strong ability to identify NTLs accurately. The testing of the method with the SGCC dataset yielded slightly weaker (but still strong) metrics, with a MAP@50 of 95.82%, a MAP@100 of 95.65%, an AUC of 96.7%, and an FPR of 8.1%.

Figure 6: The proposed method's AUC, MAP and FPR results



The method's achievement of high MAP and AUC values with both datasets indicated the effectiveness of the proposed method in detecting NTLs. In addition, the low FPR on both datasets indicated the proposed method's capacity to minimise false positives. The consistent performance across both datasets highlighted the robustness of the proposed method. The small variations between the results for the two datasets can be attributed to differences in dataset characteristics.

Performance comparison between information-fusion and stand-alone representations

To further evaluate the effectiveness of the proposed method's NTL information-fusion of features from different representations, we compared the performance of the proposed method with the stand-alone performance of each of the individual representations. The results in Tables 2 and 3 demonstrate that our proposed method's integration of features from several representations significantly improves NTL detection performance when compared with the performance of individual representations.

Table 2 shows the results for the CER dataset, with the results indicating an increase in AUC of approximately 1.4% to 3% when fusing features from CWT, MTF and raw representations compared to using them individually. Also, FPR decreases significantly, from 0.107 with raw features to 0.052 when using fused features. With respect to computational efficiency, the fused model's training time (29.41 secs) was faster than the training times for both MTF and CWT, but slower than training time (18.48 secs) for the raw 1D representation.

Table 2: NTL-detection performance comparison on CER dataset

Metrics	Raw	CWT	MTF	Fused features
AUC	0.94	0.953	0.937	0.967
MAP@100	0.954	0.965	0.969	0.973
FPR	0.107	0.073	0.071	0.052
Time (sec)	18.48	37.81	34.67	29.41

Table 3 presents the results for the SGCC dataset. Again the findings reveal a substantial improvement in detection performance, with AUC values increasing by 7.7% to 14% when transitioning from individual representations to combined features, and with FPR dropping from 0.274 to 0.081. With respect to computational efficiency, the fused model's training time (185.82 secs) was faster than the training times for CWT, but slower than training times for MTF (184.42) and for the raw 1D representation (102.51). It is worth noting that the fused-features approach required longer training times than the raw 1D representation for both datasets. However, these times remained significantly lower than those observed for CWT and MTF individually, suggesting that the fusion process optimised computational efficiency despite its added complexity.

Table 3: NTL detection performance comparison on SGCC dataset

Metrics	Raw	CWT	MTF	Fused features
AUC	0.827	0.89	0.874	0.967
MAP@100	0.87	0.894	0.888	0.957
FPR	0.274	0.218	0.253	0.081
Time (sec)	102.51	188.05	184.42	185.82

Performance comparison with existing methods

Furthermore, we compared performance of our proposed method against the performance of other methods applied to the SGCC and CER datasets. Zheng et al. (2018) implemented a wide and deep CNN using consumption patterns represented as 1D and 2D with the SGCC dataset. Also with the SGCC dataset, Shehzad et al. (2022) employed a SVM model that applied 11 features derived from the consumption pattern as the input. With EC represented as 2D matrices derived from monthly consumption data, Massaferrero et al. (2022) utilised CNN multi-resolution with the CER dataset; Nawaz et al. (2023) deployed a CNN with XGBoost for the SGCC dataset; and Xia et al. (2023) used CNN with the SGCC dataset. Bastos et al. (2023) proposed an ensemble model combining time series forest, residual network, inception time, time Le-Net, and multi-channel deep CNN, all trained on a 1D EC pattern. Since these studies used datasets similar to ours, we adopted their reported performances for initial comparison.

As shown in Table 4, our method's performance was significantly better than that of even the strongest models discussed in the literature on use of the SGCC and CER datasets, namely the Zheng et al. (2018) wide and deep CNN method, which achieved a MAP@100 of 0.95 with the SGCC dataset, and the Shehzad et al. (2022) SVM method, which achieved an AUC of 0.91 with the CER dataset.

Table 4: Method performance comparison (NTL detection in SGCC and CER datasets)

Method	Dataset	Input(s)	Metrics		
			AUC	FPR	MAP@100
wide and deep CNN (Zheng et al., 2018)	SGCC	1D and 2D	0.782		0.95
SVM (Shehzad et al., 2022)	SGCC	11 features	0.91		
CNN multi-resolution (Massaferro et al., 2022)	CER	2D	0.86		
CNN + XGBoost (Nawaz et al., 2023)	SGCC	1D and 2D	0.54		
CNN (Xia et al., 2023)	SGCC	1D and 2D	0.836		0.951
Ensemble (TSF, ResNet, Inception time, time-Le-Net, MDCNN) (Bastos et al., 2023)	CER	1D		0.016	
Our proposed method	SGCC	Fused 1D and 2D	0.967	0.081	0.957
	CER	Fused 1D and 2D	0.967	0.052	0.971

Comparison with baseline classifiers using handcrafted features

To further assess the advantages of automatic feature-learning, we compared the detection performance of our proposed method with baseline models trained on handcrafted features. The baseline models we used for the comparison were k-nearest neighbour (KNN), decision tree (DT), random forest (RF), and an SVM model. The input features for these models consisted of five handcrafted attributes per consumption pattern: four statistical measures (mean, standard deviation, variance, skewness) and one frequency-domain feature (spectral centroid) extracted from raw EC time series. Table 5 summarises the configurations and key parameters selected for model training for each baseline classifier.

Table 5: Configuration of baseline classifier models

Model	Key configuration
KNN	Number of neighbours k = 10
DT	Criterion= Gini
RF	Number of trees = 100, criterion = Gini,
SVM	Kernel = RBF, C = 1.0
Common settings	5-fold cross-validation; missing values handled using KNN imputation (k=5)

Table 6 shows the apparent advantages of our deep-learning approach (using CNN and MLP) over the handcrafted feature-engineering used in baseline models. The results show that our proposed method's achievement of an AUC of 0.967 on both datasets markedly surpassed the performance of KNN, decision tree, random forest and SVM, all of which yielded lower AUCs ranging from 0.50 to 0.84. Our proposed method also demonstrated a low FPR and a high MAP@100, indicating its ability to minimise erroneous predictions and to prioritise relevant predictions at the top of the ranked list.

Table 6: Method performance comparison (NTL detection in SGCC and CER datasets)

Baseline Method	Dataset	Inputs	AUC	FPR	MAP@100
KNN	SGCC	Handcrafted features	0.579	0.301	0.723
	CER	Handcrafted features	0.729	0.848	0.714
DT	SGCC	Handcrafted features	0.527	0.381	0.684
	CER	Handcrafted features	0.704	0.607	0.538
RF	SGCC	Handcrafted features	0.624	0.326	0.91
	CER	Handcrafted features	0.842	0.859	0.796
SVM	SGCC	Handcrafted features	0.504	0.529	0.679
	CER	Handcrafted features	0.769	0.859	0.796
Our proposed method	SGCC	Fused 1D and 2D	0.967	0.081	0.957
	CER	Fused 1D and 2D	0.967	0.052	0.971

5. Conclusions

This study has proposed and evaluated an information-fusion approach to deep-learning NTL detection in electricity grids. The key innovation of the proposed method is its ability to take advantage of various representations of EC patterns and enhance the feature-extraction capabilities of deep-learning models. The proposed model has three parallel branches that simultaneously analyse: temporal information from the MTF representation; spectral information from the CWT representation; and frequently recurring patterns in the 1D representation of raw EC data. By integrating these diverse representations, the model can sufficiently capture temporal, spectral, and periodicity information without relying on handcrafted features. Moreover, the proposed method employs deep CNN to extract features from 2D representations (using MTF and CWT) while utilising MLP to extract features from the raw 1D representation of EC data. Through our experiments on real-world datasets provided by the SGCC and CER, we found the proposed model demonstrates better NTL performance than that found in similar studies using the the same datasets. The performance and efficiency of our proposed information-fusion deep-learning network suggest a promising response to electrical utilities' need to to improve NTL detection and, in turn, to limit their grids' performance and financial losses.

Acknowledgements

We are grateful to the Irish Social Science Data Archive (ISSDA) for providing access to the CER Smart Metering Project – Electricity Customer Behaviour Trial (2009-2010) dataset, and the Kaggle repository for providing access to the State Grid Corporation of China (SGCC) dataset.

Data availability

The study used two publically available datasets to support the findings. The Irish dataset is available from the ISSDA at <https://www.ucd.ie/issda/data/commissionforenergyregulationcer/> with reference number 0012-00. The SGCC dataset is available via the Kaggle repository at <https://www.kaggle.com/datasets/bensalem14/sgcc-dataset>.

AI declaration

While preparing this work, the authors used Grammarly and online AI-assisted technologies to check grammar and spelling. After using the tools, the authors reviewed and edited the content as required and take full responsibility for the content of the publication.

Competing interests declaration

The authors have no competing interests to declare.

Authors' contributions

MGC: Conceptualisation, methodology, data collection, data analysis, validation, data curation, writing the initial draft.
 DN: Student supervision, writing – revisions.
 RM: Student supervision, writing – revisions.
 All authors read and approved the final manuscript.

References

- Adongo, C. A., Taale, F., Bukari, S., Suleman, S., & Amadu, I. (2021). Electricity theft whistleblowing feasibility in commercial accommodation facilities. *Energy Policy*, 155, 112347. <https://doi.org/10.1016/j.enpol.2021.112347>
- Bai, Y., Sun, H., Zhang, L., & Wu, H. (2023). Hybrid CNN-transformer network for electricity theft detection in smart grids. *Sensors*, 23(20), 1–21. <https://doi.org/10.3390/s23208405>
- Bastos, L., Pfeiff, G., Oliveira, R., Oliveira, H., Tostes, M. E., Zeadally, S., Cerqueira, E., & Rosário, D. (2023). Data-oriented ensemble predictor based on time series classifiers for fraud detection. *Electric Power Systems Research*, 223(July), 109547. <https://doi.org/10.1016/j.epsr.2023.109547>
- Boashash, B. (2009). Time-frequency and instantaneous frequency concepts. In *Time-frequency signal analysis and processing: A comprehensive reference* (pp. 31–61). Academic Press.
- Chawla, N. V., Bowyer, K. W., & Hall, L. O. (2002). SMOTE : Synthetic Minority Over-sampling Technique. *Journal of Artificial Intelligence Research*, 16, 321–357. <https://doi.org/10.1613/jair.953>
- Chen, J., Nanekaran, Y. A., Chen, W., Liu, Y., & Zhang, D. (2023). Data-driven intelligent method for detection of electricity theft. *International Journal of Electrical Power and Energy Systems*, 148(September), 108948. <https://doi.org/10.1016/j.ijepes.2023.108948>
- Chen, V. C., & Ling, H. (2002). *Time-frequency transforms for radar imaging and signal analysis*. Artech House.
- Chen, Y., Li, J., Huang, Q., Li, K., Zhao, Z., & Ren, X. (2023). Non-technical losses detection with Gramian angular field and deep residual network. *The 3rd International Conference on Power and Electrical Engineering, Energy Reports*, 9, 1392–1401. <https://doi.org/10.1016/j.egyr.2023.05.183>
- Chuwa, M. G., & Wang, F. (2021). A review of non-technical loss attack models and detection methods in the smart grid. *Electric Power Systems Research*, 199, 107415. <https://doi.org/10.1016/J.EPSR.2021.107415>
- Commission for Energy Regulation (CER). (2012). *CER Smart Metering Project - Electricity Customer Behaviour Trial, 2009-2010* [Dataset]. Irish Social Science Data Archive. SN: 0012-00. <https://www.ucd.ie/issda/accessdata/issdadatasets>
- Fang, H., Xiao, J. W., & Wang, Y. W. (2023). A machine learning-based detection framework against intermittent electricity theft attack. *International Journal of Electrical Power and Energy Systems*, 150(February), 109075. <https://doi.org/10.1016/j.ijepes.2023.109075>
- Guarda, F. G. K., Hammerschmitt, B. K., Capeletti, M. B., Neto, N. K., dos Santos, L. L. C., Prade, L. R., & Abaide, A. (2023). Non-hardware-based non-technical losses detection methods: A review. *Energies*, 16(4), 1–27. <https://doi.org/10.3390/en16042054>
- Haq, E. U., Pei, C., Zhang, R., Jianjun, H., & Ahmad, F. (2023). Electricity-theft detection for smart grid security using smart meter data: A deep-CNN based approach. *Energy Reports*, 9, 634–643. <https://doi.org/10.1016/j.egyr.2022.11.072>
- Javaid, N., Jan, N., & Javed, M. U. (2021). An adaptive synthesis to handle imbalanced big data with deep siamese network for electricity theft detection in smart grids. *Journal of Parallel and Distributed Computing*, 153, 44–52. <https://doi.org/10.1016/j.jpdc.2021.03.002>
- Jokar, P., Arianpoo, N., & Leung, V. C. M. (2016). Electricity theft detection in AMI using customers' consumption patterns. *IEEE Transactions on Smart Grid*, 7(1), 216–226. <https://doi.org/10.1109/TSG.2015.2425222>
- Khan, Z. A., Adil, M., Javaid, N., Saqib, M. N., Shafiq, M., & Choi, J. G. (2020). Electricity theft detection using supervised learning techniques on smart meter data. *Sustainability*, 12(19), 1–25. <https://doi.org/10.3390/su12198023>
- Liao, W., Yang, Z., Liu, K., Zhang, B., Chen, X., & Song, R. (2023). Electricity theft detection using Euclidean and graph convolutional neural networks. *IEEE Transactions on Power Systems*, 38(4), 3514–3527. <https://doi.org/10.1109/TPWRS.2022.3196403>
- Massaferro, P., Di Martino, J. M., & Fernandez, A. (2022). Fraud detection on power grids while transitioning to smart meters by leveraging multi-resolution consumption data. *IEEE Transactions on Smart Grid*, 3053(c), 1–10. <https://doi.org/10.1109/TSG.2022.3148817>
- Nawaz, A., Ali, T., Mustafa, G., Rehman, S. U., & Rashid, M. R. (2023). A novel technique for detecting electricity theft in secure smart grids using CNN and XG-boost. *Intelligent Systems with Applications*, 17, 200168. <https://doi.org/10.1016/j.iswa.2022.200168>

- Pan, H., Feng, X., Na, C., & Yang, H. (2023). A model for detecting false data injection attacks in smart grids based on the method utilized for image coding. *IEEE Systems Journal*, 17(4), 6181–6191. <https://doi.org/10.1109/JSYST.2023.3287924>
- Pereira, J., & Saraiva, F. (2021). Convolutional neural network applied to detect electricity theft: A comparative study on unbalanced data handling techniques. *International Journal of Electrical Power and Energy Systems*, 131(March), 107085. <https://doi.org/10.1016/j.ijepes.2021.107085>
- Shehzad, F., Javaid, N., Aslam, S., & Umar Javaid, M. (2022). Electricity theft detection using big data and genetic algorithm in electric power systems. *Electric Power Systems Research*, 209(October 2021), 107975. <https://doi.org/10.1016/j.epsr.2022.107975>
- Shi, J., Gao, Y., Gu, D., Li, Y., & Chen, K. (2023). A novel approach to detect electricity theft based on conv-attentional Transformer Neural Network. *International Journal of Electrical Power and Energy Systems*, 145(February), 10862. <https://doi.org/10.1016/j.ijepes.2022.108642>
- Wang, Z., & Oates, T. (2015). *Spatially encoding temporal correlations to classify temporal data using convolutional neural networks*. <http://arxiv.org/abs/1509.07481>
- Xia, R., Gao, Y., Zhu, Y., Gu, D., & Wang, J. (2023). An attention-based wide and deep CNN with dilated convolutions for detecting electricity theft considering imbalanced data. *Electric Power Systems Research*, 214, 108886. <https://doi.org/10.1016/j.epsr.2022.108886>
- Yan, Z., Member, S., Wen, H., & Member, S. (2022). Performance analysis of electricity theft detection for the smart grid: An overview. *IEEE Transactions on Instrumentation and Measurement*, 71. <https://doi.org/10.1109/TIM.2021.3127649>
- Zheng, Z., Yang, Y., Niu, X., Dai, H. N., & Zhou, Y. (2018). Wide and deep convolutional neural networks for electricity-theft detection to secure smart grids. *IEEE Transactions on Industrial Informatics*, 14(4), 1606–1615. <https://doi.org/10.1109/TII.2017.2785963>
- Zidi, S., Mihoub, A., Mian Qaisar, S., Krichen, M., & Abu Al-Haija, Q. (2023). Theft detection dataset for benchmarking and machine learning based classification in a smart grid environment. *Journal of King Saud University - Computer and Information Sciences*, 35(1), 13–25. <https://doi.org/10.1016/j.jksuci.2022.05.007>